

Spatio-Temporal Analysis of Sea Level Pressure and Surface Temperature Dynamics Using Data-Driven Methods

Praveen Kumar Krishnapur^a

^aDepartment of Mechanical Engineering, National University of Singapore, Singapore

This manuscript was compiled on April 21, 2025

This study investigates the spatio-temporal dynamics of Sea Level Pressure (SLP) and Two-Meter Temperature (T2M) over the Indo-Pacific region from 1979 to 2022 using a suite of data-driven techniques. Fast Fourier Transform (FFT) (1) reveals dominant seasonal periodicities in the averaged time series, while Singular Value Decomposition (SVD) (2, 3) identifies the most energetic spatial modes, enabling reduced-order representation. Dynamic Mode Decomposition (DMD) (4) is employed on the top SVD modes to extract temporally evolving coherent structures and forecast future states based on a linear evolution model. To address the limitations of linearity in DMD, a feed-forward neural network (NN) (5) is trained on the same reduced feature space to capture nonlinear dynamics. Predictions are carried out for the period 2020–2022 and evaluated across both methods. Despite their structural differences, DMD and NN yield comparable root mean squared errors (472.4 Pa vs. 472.1 Pa), largely due to the use of identical dominant modes capturing 99% of system energy. However, analysis of spatial error distributions and long-horizon predictions reveals that NN better captures nonlinear residuals in dynamically active regions. This work demonstrates that reduced-order modeling paired with learning-based methods can effectively balance interpretability and predictive accuracy for atmospheric data.

Fast Fourier Transform (FFT) | Singular Value Decomposition (SVD) | Reduced-order Modelling | Dynamic Mode Decomposition (DMD) | Neural Networks (NN)

Introduction

Understanding climate dynamics is essential for anticipating and mitigating the effects of extreme weather events, long-term climate change, and their associated socio-economic impacts. The Earth's climate system is inherently multi-scale, high-dimensional, nonlinear, and chaotic, posing significant challenges for analysis while offering rich opportunities for data-driven exploration.

This study focuses on a high-resolution spatio-temporal dataset derived from reanalysis products, spanning the Indo-Pacific region from 1979 to 2022. The dataset includes daily measurements of two fundamental atmospheric variables: sea level pressure (SLP) and two-meter temperature (T2M), with a spatial resolution of $0.5^\circ \times 0.5^\circ$. Each time snapshot comprises 16,261 grid points, resulting in a total of 16,071 temporal instances.

To extract meaningful patterns and investigate the dynamics underlying the system's evolution, a series of data-driven techniques are employed—specifically Fast Fourier Transform (FFT), Singular Value Decomposition (SVD), Dynamic Mode Decomposition (DMD), and Neural Networks (NN). These tools facilitate the identification of both spatial and temporal features present in the data.

The objective is to evaluate the potential of reduced-order models to represent the observed dynamics and to assess the feasibility of short-term forecasting. While linear methods such as DMD are utilized to extract coherent structures and dominant modes, neural networks offer a nonlinear modeling framework capable of capturing more complex behaviors, though subject to limitations imposed by the chaotic nature of the climate system.

Fast Fourier Transform (FFT). The Fast Fourier Transform (FFT) is an efficient algorithm for computing the Discrete Fourier Transform (DFT) of a signal. It decomposes a time-domain signal into a set of sinusoidal components, revealing the strength of various frequency contributions. Mathematically, the DFT of a discrete signal $x(n)$ of length N is given by:

$$X(k) = \sum_{n=0}^{N-1} x(n)e^{-j2\pi kn/N}, \quad k = 0, 1, \dots, N-1$$

To analyze the temporal behavior of the Sea Level Pressure (SLP) field, the spatial average of SLP was computed over the Indo-Pacific region, followed by temporal averaging over non-overlapping three-month intervals. This produced a one-dimensional time series capturing coarse-grained seasonal dynamics.

After detrending to eliminate long-term bias, FFT was applied to this series to identify dominant frequencies. The resulting power spectrum exhibits a sharp and isolated peak at a normalized frequency of 0.25 cycles/sample, corresponding to a periodicity of four time steps (12 months) —equivalent to one year. This clearly indicates a strong and recurring annual cycle.

No other frequency in the spectrum exhibits comparable magnitude, highlighting the dominance of the annual cycle over other intra- or inter-seasonal fluctuations. This observation is particularly significant in the Indo-Pacific region, where the seasonal reversal of monsoon winds and thermal gradients between ocean and land strongly influence the atmospheric pressure fields. The clarity and strength of the annual signal suggest that the large-scale atmospheric dynamics in this region are tightly governed by seasonal forcing mechanisms, making the annual cycle the primary mode of variability.

This dominant periodicity is clearly visible in Figure 1a,b, reinforcing its role as the principal temporal structure in the evolution of SLP over the Indo-Pacific basin.

Singular Value Decomposition (SVD). Singular Value Decomposition (SVD) is a foundational linear algebra technique that factorizes a data matrix into three components: spatial modes, temporal coefficients, and a diagonal matrix of singular values. It is widely used for data compression, noise reduction, and, more importantly, for reduced-order modeling (6) of high-dimensional systems.

In the context of climate data, SVD facilitates the identification of dominant patterns by isolating the most energetic structures in both space and time. The original data matrix is approximated as a low-rank product of a reduced number of modes, significantly lowering computational complexity while preserving the system's essential dynamics.

To determine the number of modes required to capture the core dynamics, SVD was applied separately to daily Sea Level Pressure (SLP) and Two-Meter Temperature (T2M) data over four distinct decades. The three-dimensional spatio-temporal dataset was reshaped into a two-dimensional matrix of spatial points versus time and was centered by subtracting the temporal mean at each spatial location.

The singular values resulting from the decomposition quantify the energy captured by each mode. The cumulative energy spectrum (see Figure 1c,d) was used to identify the number of modes necessary to retain 99% of the total system energy. These results are presented in Table 1.

Table 1. Number of SVD modes retaining 99% of energy per decade

Decade	SLP Modes	T2M Modes
1980–1989	60	117
1990–1999	61	122
2000–2009	61	128
2010–2019	64	124

As the objective is to assess recent climatic behavior, the analysis focuses on the most recent decade (2010–2019). During this period, 64 modes are sufficient to retain 99% of the energy in the SLP field, while 124 modes are required for the T2M field. This indicates that temperature exhibits greater spatial-temporal variability than pressure, necessitating a higher-dimensional representation for accurate modeling. The disparity underscores the added complexity involved in modeling temperature dynamics, which may influence the selection of reduced-order model configurations and forecasting methodologies.

Dynamic Mode Decomposition (DMD). Dynamic Mode Decomposition (DMD) is a data-driven technique for modeling the temporal evolution of complex systems (4). It approximates the dynamics as a linear transformation acting on spatial modes, which enables reduced-order forecasting and dynamic characterization. The method begins with constructing two data matrices from sequential time snapshots:

$$\mathbf{X} = [\mathbf{x}_1 \quad \mathbf{x}_2 \quad \cdots \quad \mathbf{x}_{m-1}], \quad \mathbf{X}' = [\mathbf{x}_2 \quad \mathbf{x}_3 \quad \cdots \quad \mathbf{x}_m]$$

The goal is to approximate the linear mapping between snapshots as:

$$\mathbf{X}' \approx \mathbf{A}\mathbf{X}$$

Since the original system is typically high-dimensional, a truncated Singular Value Decomposition (SVD) (2) is performed on \mathbf{X} :

$$\mathbf{X} \approx \mathbf{U}_r \mathbf{\Sigma}_r \mathbf{V}_r^*$$

where r is the number of retained modes (e.g., 64 for SLP), and \mathbf{U}_r represents the dominant spatial structures. The reduced system operator $\tilde{\mathbf{A}}$ is then computed as:

$$\tilde{\mathbf{A}} = \mathbf{U}_r^* \mathbf{X}' \mathbf{V}_r \mathbf{\Sigma}_r^{-1}$$

An eigendecomposition is performed on $\tilde{\mathbf{A}}$:

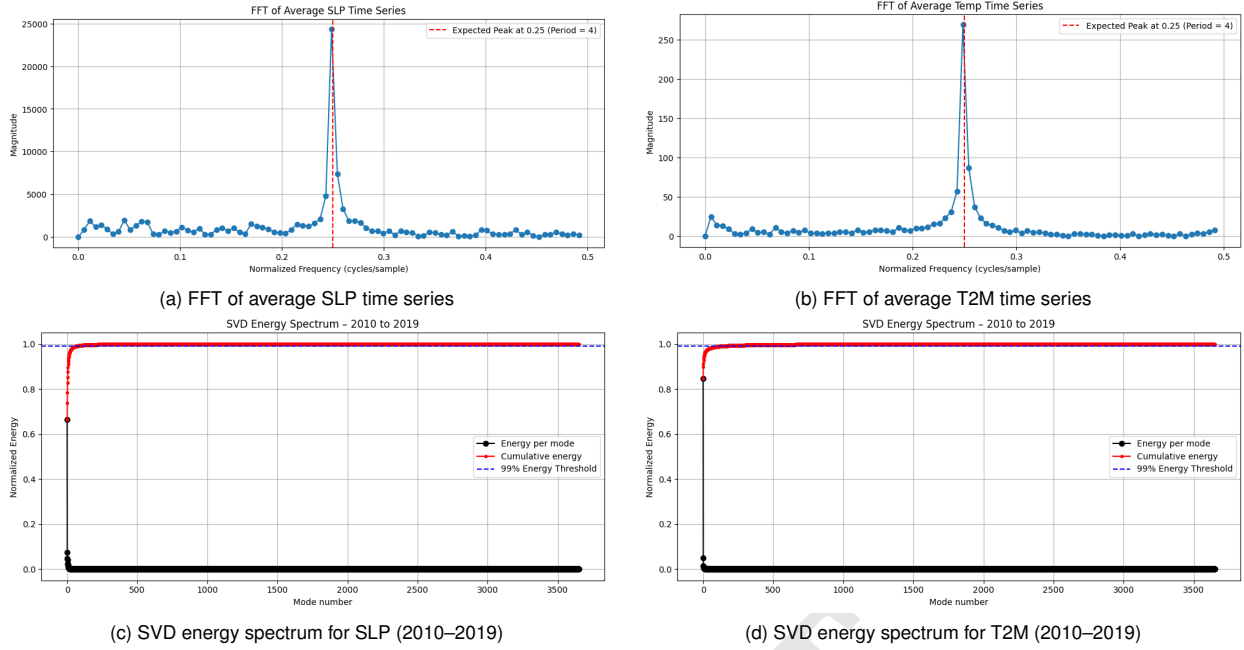


Fig. 1. Comparison of dominant frequency and energy modes for SLP and T2M. FFT plots reveal strong seasonal signals, while SVD plots highlight the number of modes required to retain 99% of system energy in the last decade.

$$\tilde{\mathbf{A}}\mathbf{W} = \mathbf{W}\mathbf{A}$$

The DMD modes Φ , which describe the dominant spatial structures evolving linearly in time, are computed as:

$$\Phi = \mathbf{X}'\mathbf{V}_r\mathbf{\Sigma}_r^{-1}\mathbf{W}$$

In this study, DMD is applied to the reduced SVD space derived from daily Sea Level Pressure (SLP) data over the decade 2010–2019. The top 64 SVD modes are retained to reduce dimensionality while capturing 99% of the total system energy. This projection significantly lowers computational cost and enables meaningful analysis in a reduced-order space.

The DMD eigenvalue spectra, shown in Figure 2a, display the distribution of Ritz values across four decades. Their location in the complex plane determines the temporal characteristics of the corresponding modes, as summarized in Table 2.

Table 2. Interpretation of DMD Eigenvalue Locations in the Complex Plane

Eigenvalue Location	Interpretation
$ \lambda = 1$ (unit circle)	Purely periodic mode (no growth or decay)
$ \lambda < 1$ (inside unit circle)	Decaying mode (energy loss over time)
$ \lambda > 1$ (outside unit circle)	Growing/unstable mode (not observed here)
Real axis	Non-oscillatory exponential behavior
Imaginary axis	Strongly oscillatory with minimal decay/growth

The majority of the Ritz values lie well inside the unit circle, indicating a generally stable system with weakly decaying modes. A tight clustering near (1,0) suggests the presence of persistent but non-oscillatory structures—coherent patterns that change slowly over time. Only a sparse distribution of complex conjugate eigenvalues implies limited presence of oscillatory or wave-like behavior within the observed climate dynamics.

To further interpret the spatio-temporal behavior of the system, the leading DMD modes for both SLP and Two-Meter Temperature (T2M) are extracted and shown in Figure 2b and Figure 2c, respectively. These dominant modes highlight the spatial regions most responsible for the system's temporal evolution.

A few key conclusions can be drawn:

- For both SLP and T2M, **the most dominant dynamic modes are concentrated in the northeastern sector** of the domain, particularly over regions such as the East China Sea, the western Pacific, and parts of East Asia. This indicates that these regions exhibit strong temporal variability and potentially contribute to seasonal-scale transitions or local weather systems.
- In contrast, **the equatorial region appears spatially quiescent** in both datasets. This aligns with known climate dynamics in the equatorial Indo-Pacific, where certain structures exhibit relative spatial stationarity and slow temporal evolution.

****T2M modes display sharper and more localized gradients**** compared to SLP, reinforcing earlier observations from SVD that temperature fields require more modes to represent their variability. This may result from stronger land-sea contrasts and more localized heat dynamics in surface temperature fields. - The DMD mode amplitudes are also more intense in the T2M field, particularly around 20°N to 35°N, indicating regions where temperature fluctuations play a dominant role in short-term dynamics.

These dominant modes serve as the building blocks of the reduced-order linear model formed by DMD. Each mode evolves over time according to its associated eigenvalue and can be linearly combined to reconstruct or forecast future system states. While effective for low-dimensional linear dynamics, the inherent linearity of DMD limits its ability to fully capture nonlinear behaviors—hence motivating the use of more flexible models such as neural networks (NN), discussed in the following section.

The next section evaluates the predictive performance of the DMD-based linear model and compares it with a neural network trained to learn nonlinear mappings in the same reduced space.

Future Prediction

Using DMD. Once the dynamic modes and eigenvalues of a system have been extracted via DMD, they can be used to forecast the system’s evolution. The state of the system at any future time t can be reconstructed using the DMD formulation:

$$\mathbf{x}(t) = \sum_{k=1}^r b_k \phi_k e^{\omega_k t}$$

where: - ϕ_k are the DMD modes, - $\omega_k = \ln(\lambda_k)/\Delta t$ are the continuous-time eigenvalues, - b_k are the mode amplitudes computed from the initial condition, - r is the number of retained modes (here, $r = 64$), - λ_k are the discrete-time Ritz eigenvalues.

This equation allows the system to evolve forward in time using a reduced number of dominant spatio-temporal structures. The exponential term $e^{\omega_k t}$ governs each mode’s growth, decay, or oscillatory behavior.

In this analysis, DMD was applied to Sea Level Pressure (SLP) data, with the model trained on the decade from January 1, 2010 to December 31, 2019. The system was projected onto 64 dominant SVD modes, capturing 99% of the total energy. Using this reduced-order representation, future states were predicted over the next three-year window, from January 1, 2020 to December 31, 2022. While this methodology is generalizable to other fields such as Two-Meter Temperature (T2M), the focus here is limited to SLP.

To qualitatively assess predictive performance, Table 4 compares predicted and actual SLP values at 10 selected spatial points on the first forecast day. Similarly, Table 5 presents the same comparison for the final time step of the test period. These snapshots highlight the model’s ability to capture short-term dynamics while also revealing limitations due to long-term linear propagation.

Additionally, the Mean Absolute Error (MAE) distribution for DMD predictions across the 2020–2022 period is shown in Figure 2f. The error is concentrated predominantly in the northern regions of the domain, while the equatorial regions exhibit very low MAE. This spatial pattern aligns well with earlier observations from the dominant DMD modes: minimal spatio-temporal coherence was detected near the equator, implying relatively stable atmospheric behavior. As a result, DMD models achieve higher accuracy in these regions, due to the reduced variability in underlying dynamics.

Using Neural Networks. Neural Networks (NNs) are a class of flexible function approximators inspired by the biological nervous system. They are particularly powerful in capturing nonlinear relationships between inputs and outputs, making them suitable for modeling complex dynamical systems where linear models like DMD may fall short. Over the last decade, Deep Neural Networks (DNNs) have found widespread applications in fields ranging from image classification and natural language processing to physics-informed modeling and climate prediction.

In contrast to the linear assumption underlying DMD, NNs do not impose any specific structural form on the dynamics and can learn arbitrary nonlinear mappings from training data. This makes them a natural candidate for modeling residual dynamics or capturing features not resolved by linear methods.

Modeling Strategy and Architecture. To ensure a fair comparison with the DMD framework, we retain the same reduced-order feature space. Specifically, the SLP field from 2010–2019 is reshaped into a matrix of size (space, time), and the temporal mean is subtracted at each spatial point. We apply Truncated SVD and retain the top 64 modes, resulting in modal coefficients that represent the reduced dynamics. These 64 features serve as the input and output dimensions of the neural network.

The temporal evolution is learned as a one-step prediction problem: given the modal coefficients $\alpha(t)$, the network predicts $\alpha(t + 1)$. To stabilize training, the input and output coefficients are normalized using standard scaling (zero mean and unit variance across each mode). The architecture of the neural network used for this prediction task is summarized in Table 3.

ReLU (Rectified Linear Unit) activation functions were chosen for their simplicity and effectiveness in handling nonlinearity while avoiding vanishing gradients. The use of 64 features ensures direct comparability with the DMD model, where the same number of modes was used.

Table 3. Neural Network Architecture for Modal Forecasting

Layer Type	Details
Input Layer	64 neurons (modal coefficients)
Hidden Layer 1	128 neurons, ReLU activation
Hidden Layer 2	128 neurons, ReLU activation
Hidden Layer 3	64 neurons, ReLU activation
Output Layer	64 neurons (forecasted modal coefficients)

Training Details. The network was trained on normalized modal coefficient pairs $(\alpha(t), \alpha(t+1))$ derived from the decade 2010–2019. Initial experimentation with the Adam optimizer(7) enabled fast convergence but led to overfitting on the training data. To mitigate this, the model was subsequently retrained using Stochastic Gradient Descent (SGD) with momentum and weight decay as regularization strategies (8) . Optimization was performed using Mean Squared Error (MSE) loss over a total of 1,000 training epochs.

Training was conducted on GPU using PyTorch. After training, recursive multi-step prediction was performed: the model predicted one time step at a time, using its previous output as the next input. This process was repeated across the test period (January 1, 2020 to December 31, 2022).

The predicted modal coefficients were then transformed back to physical space using the inverse SVD transform, followed by re-adding the mean field.

To evaluate the NN’s predictive performance, we compare its results to those of the DMD model over the same time window. Table 4 shows the predicted and actual values for the **first 10 spatial points at the first time step** of 2020. Similarly, Table 5 shows the predicted and actual values for the **same 10 spatial points at the final time step** of 2022.

Table 4. Comparison of Actual, DMD, and NN Predicted SLP Values on 2020-01-01 for 10 Spatial Points

Index	Date	Latitude	Longitude	Actual (Pa)	Predicted_DMD (Pa)	Predicted_NN (Pa)
1	2020-01-01	40.0	70.0	101887.96	101667.16	101979.05
2	2020-01-01	40.0	70.5	101958.42	101704.66	102023.76
3	2020-01-01	40.0	71.0	101970.90	101720.97	102036.66
4	2020-01-01	40.0	71.5	101868.62	101757.10	101970.70
5	2020-01-01	40.0	72.0	101849.70	101775.80	101950.30
6	2020-01-01	40.0	72.5	101873.83	101927.29	101975.75
7	2020-01-01	40.0	73.0	101978.98	101940.24	102009.38
8	2020-01-01	40.0	73.5	102160.23	101975.40	102070.61
9	2020-01-01	40.0	74.0	102553.49	102110.50	102302.48
10	2020-01-01	40.0	74.5	102577.13	102042.89	102367.34

Table 5. Comparison of Actual, DMD, and NN Predicted SLP Values on 2022-12-22 for 10 Spatial Points

Index	Date	Latitude	Longitude	Actual (Pa)	Predicted_DMD (Pa)	Predicted_NN (Pa)
1	2022-12-22	40.0	70.0	103110.06	101667.16	101618.54
2	2022-12-22	40.0	70.5	103050.55	101704.66	101657.67
3	2022-12-22	40.0	71.0	103079.84	101720.97	101674.47
4	2022-12-22	40.0	71.5	102957.41	101757.10	101714.52
5	2022-12-22	40.0	72.0	102936.38	101775.80	101735.71
6	2022-12-22	40.0	72.5	102895.09	101927.29	101892.97
7	2022-12-22	40.0	73.0	102897.20	101940.24	101906.71
8	2022-12-22	40.0	73.5	102905.91	101975.40	101941.70
9	2022-12-22	40.0	74.0	102997.85	102110.50	102076.91
10	2022-12-22	40.0	74.5	102866.51	102042.89	102011.00

Comparison of NN and DMD. Both DMD and Neural Networks (NN) demonstrate competitive performance in forecasting sea level pressure (SLP) over the test period from January 1, 2020 to December 31, 2022. The overall root mean squared error (RMSE) across this three-year span is remarkably similar for the two models:

- DMD RMSE for 2020–2022 prediction: **472.43 Pa**
- NN RMSE for 2020–2022 prediction: **472.13 Pa**

This similarity is further evident in the RMSE histograms shown in Figure 2d,e, where both models exhibit comparable error distributions consistent with the average RMSE values. This near equivalence in performance arises from two key factors. First, the temporal evolution of the dominant modes over short time intervals tends to be largely linear, making it possible for DMD—a fundamentally linear model—to perform well. Second, both models were trained using the same reduced feature space: the top 64 SVD modes, which together capture approximately 99% of the total energy in the system. These modes encapsulate the most significant spatial-temporal patterns, leaving little residual dynamics for either model to improve upon.

However, if a lower-rank approximation were used in DMD—say, retaining only 20–30 modes (around 70% of the energy)—while allowing the neural network to access the full high-dimensional space, we would expect the NN to outperform DMD due to its capacity to model complex, nonlinear interactions. This underscores that the comparable performance in our current setup is largely a result of how the input data was curated and preprocessed, rather than an inherent limitation or superiority of either modeling approach.

A closer inspection of prediction accuracy at specific time points highlights a subtle but important trend:

- At the **first time step** (2020-01-01), DMD slightly outperforms NN:

- DMD RMSE: **1203.88 Pa**

- NN RMSE: **1243.85 Pa**

- At the **last time step** (2022-12-22), NN outperforms DMD:

- DMD RMSE: **204.17 Pa**

- NN RMSE: **122.38 Pa**

These findings suggest that while DMD excels in short-term prediction due to its efficient propagation of dominant modes, its linear assumptions become limiting over longer time horizons. As the forecast horizon extends, nonlinear effects—such as residual dynamics, mode interactions, and local disturbances—become more significant. NN models, with their ability to capture nonlinear mappings, gradually surpass DMD in accuracy as time progresses.

In future work, a promising extension would involve training neural networks on the full spatial-temporal dataset rather than a truncated set of modes. This would allow the network to learn directly from both high- and low-energy structures, potentially improving its ability to capture subtle nonlinearities that are lost during dimensionality reduction. Additionally, hybrid approaches could be explored—where DMD captures dominant linear trends and NN models the nonlinear residual—offering a best-of-both-worlds framework for spatio-temporal prediction.

Conclusion. This study applied a sequence of data-driven techniques to investigate the spatio-temporal behavior of Sea Level Pressure (SLP) and Two-Meter Temperature (T2M) over the Indo-Pacific region. Fast Fourier Transform (FFT) revealed a dominant annual periodicity, emphasizing the strong seasonal forcing present in this climate system. Singular Value Decomposition (SVD) enabled the extraction of dominant spatial modes, with SLP requiring fewer modes than T2M to retain 99% of system energy, indicating greater spatial-temporal variability in temperature fields.

Dynamic Mode Decomposition (DMD) was used to construct a reduced-order linear model for forecasting SLP. The model performed well in the short term due to the linear evolution of the dominant modes. A feed-forward Neural Network (NN) trained on the same reduced-order feature space demonstrated slightly better long-term accuracy, particularly in dynamically active regions, owing to its capacity to capture nonlinear dynamics.

Both DMD and NN achieved similar overall root mean squared errors over the prediction period 2020–2022. However, error distribution and end-of-horizon metrics indicated that the NN provided a more accurate reconstruction in regions of high variability. These findings suggest that while DMD offers interpretability and efficiency, neural networks present a robust complementary tool, particularly for capturing complex, non-linear behavior. Future work could explore hybrid models or training NN directly on full-resolution fields to further enhance predictive performance.

ACKNOWLEDGMENTS. I would like to sincerely thank Dr. Gianmarco Mengaldo and the course teaching assistants for their guidance and support on this project. I am also grateful to my fellow course mates for the insightful discussions and exchange of ideas that enriched the learning process. Finally, I would like to express my deepest gratitude to my parents for their unwavering support and encouragement over the years.

References. (9)

1. SL Brunton, JN Kutz, *Data-Driven Science and Engineering: Machine Learning, Dynamical Systems, and Control*. (Cambridge University Press), (2019).
2. GH Golub, C Reinsch, Singular value decomposition and least squares solutions. *Numer. Math.* **14**, 403–420 (1970).
3. CR Harris, KJ Millman, SJ van der Walt, et al., *numpy.linalg.svd*, (2020) <https://numpy.org/doc/stable/reference/generated/numpy.linalg.svd.html>.
4. PJ Schmid, Dynamic mode decomposition of numerical and experimental data. *J. fluid mechanics* **656**, 5–28 (2010).
5. A Paszke, et al., Pytorch: An imperative style, high-performance deep learning library (<https://pytorch.org>) (2019) NeurIPS 2019.
6. SL Brunton, JN Kutz, Data-driven methods for reduced-order modeling in *Model Reduction and Approximation: Theory and Algorithms*, eds. P Benner, A Cohen, M Ohlberger, K Willcox. (De Gruyter, Berlin, Boston), pp. 307–344 (2021).
7. DP Kingma, J Ba, Adam: A method for stochastic optimization. *arXiv preprint arXiv:1412.6980* (2014).
8. DE Rumelhart, GE Hinton, RJ Williams, Learning representations by back-propagating errors. *Nature* **323**, 533–536 (1986).
9. C Chung, Nus me5311 - climate data project (<https://github.com/chesterchung1998/NUS-5311>) (2024).

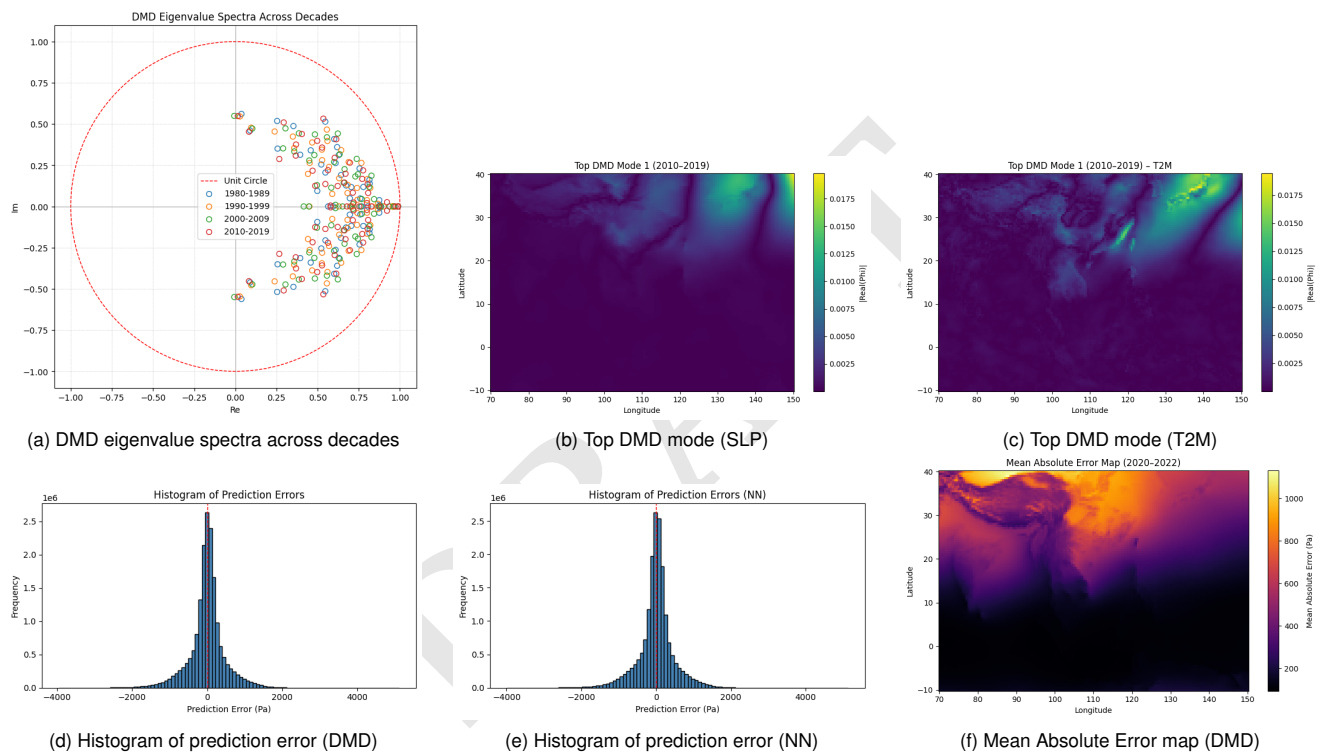


Fig. 2. Comparison of DMD and NN modeling performance. Subfigures show dynamic mode structure, eigenvalue distribution, prediction error distributions, and spatial error maps for NN.